

Temperature Dependence of the Evaporation Coefficient of Water in Air and Nitrogen under Atmospheric Pressure: Study in Water Droplets

M. Zientara, D. Jakubczyk,* K. Kolwas, and M. Kolwas

Institute of Physics of the Polish Academy of Sciences Al.Lotników 32/46, 02-668 Warsaw, Poland

Received: December 4, 2007; Revised Manuscript Received: March 4, 2008

The evaporation coefficients of water in air and nitrogen were found as a function of temperature by studying the evaporation of a pure water droplet. The droplet was levitated in an electrodynamic trap placed in a climatic chamber maintaining atmospheric pressure. Droplet radius evolution and evaporation dynamics were studied with high precision by analyzing the angle-resolved light scattering Mie interference patterns. A model of quasi-stationary droplet evolution accounting for the kinetic effects near the droplet surface was applied. In particular, the effect of thermal effusion (a short-range analogue of thermal diffusion) was discussed and accounted for. The evaporation coefficient α in air and in nitrogen were found to be equal. The α was found to decrease from ~ 0.18 to ~ 0.13 for the temperature range from 273.1 to 293.1 K and follow the trend given by the Arrhenius formula. The agreement with condensation coefficient values obtained with an essentially different method by Li et al. [Li, Y.; Davidovits, P.; Shi, Q.; Jayne, J.; Kolb, C.; Worsnop, D. *J. Phys. Chem. A* 2001, 105, 10627] was found to be excellent. The comparison of experimental conditions used in both methods revealed no dependence of the evaporation/condensation coefficient on the droplet charge nor the ambient gas pressure within the experimental parameters range. The average value of the thermal accommodation coefficient over the same temperature range was found to be 1 ± 0.05 .

1. Introduction

Many problems of science and technology are related to the evaporation from droplets and condensation on them. Cloud and aerosol microphysics together with the construction of climate models,^{2–4} electrospraying,⁵ combustion,⁶ jet printing (compare with ref 7), and spray painting (compare with ref 8) are just some areas of relevance. Though they concern large sets of coexisting droplets, the understanding of transport processes at the surface of a single droplet is vital for solving them properly. Mass and heat transport processes at the (nearly) flat interface can be efficiently modeled as a diffusion phenomenon. However, the evolution of small droplets is significantly influenced by effusion, which takes place in an effectively collision-free region in the very vicinity of the interface (up to the mean free path of surrounding gas molecules). In order to account for this phenomenon, a so-called evaporation (condensation) or mass accommodation coefficient α is introduced besides the diffusion coefficient. Likewise, the thermal conductivity coefficient should be accompanied by a thermal accommodation coefficient α_T . These coefficients describe transport properties of the liquid–gas interface. The mass accommodation coefficient can be perceived as the probability that a molecule (e.g., water) impinging on the interface from the gaseous phase side enters into the liquid phase and does not rebound. Analogically, the thermal accommodation coefficient determines the probability that a molecule impinging on the interface attains thermal equilibrium with the medium on the opposite side. The considerations of evaporation and condensation coefficients are considered to be equivalent, and the values of these coefficients are considered to be equal.⁹ Both α and α_T coefficients are phenomenological and should describe only the properties of the very interface. All other processes influencing mass and heat transport, such as the

chemistry of the interface or the electrostatic interactions, should be accounted for separately.¹⁰ It is agreed, however, that α might possibly exhibit some temperature dependence.^{9,11}

Many attempts have been made over nearly a century to determine experimentally the values of α and α_T for water, but the results obtained by different authors spanned from ~ 0.001 to 1 for α and from ~ 0.5 to 1 for α_T (see, e.g., refs 1, 12–19 and 9, 11, 20 for reviews). A variety of experimental methods was used. Both condensation on and evaporation from the surface of bulk liquid, liquid films, jets, and droplets were investigated in various environments (vacuum, standard air, passive or reactive atmospheres) under various pressures and for various water vapor saturations. Small droplets, such as those encountered in clouds, have been favored since kinetic effects manifest strongly for them. Suspended droplets, trains of droplets, clouds of droplets, and single trapped droplets were studied.

We must admit that in our studies we have also experienced the flow of kinetic coefficients values in time. We have tried to overcome it. We will discuss the possible sources of the divergence of results in section 5.1.

The measurement of the temperature dependence of α was rarely attempted since the large divergence of obtained α values obscures the effect. Two recent studies by Li et al.¹ and by Winkler et al.¹² can serve as an example. The authors of the first study (Boston College/Aerodyne Research Inc. group) found that α decreases with temperature within the temperature range between 257 and 280 K. The authors of the second study (University of Vienna/University of Helsinki group) claim that α and α_T exhibit no temperature dependence between 250 and 290 K. The comparison of these results can be found in ref 20.

In this paper, we present our new experimental results of the evaporation coefficient of water in air, as well as our reprocessed results for water in nitrogen (compare with ref 21), versus temperature, both under atmospheric pressure. The results for

* To whom correspondence should be addressed. E-mail: jakub@ifpan.edu.pl.

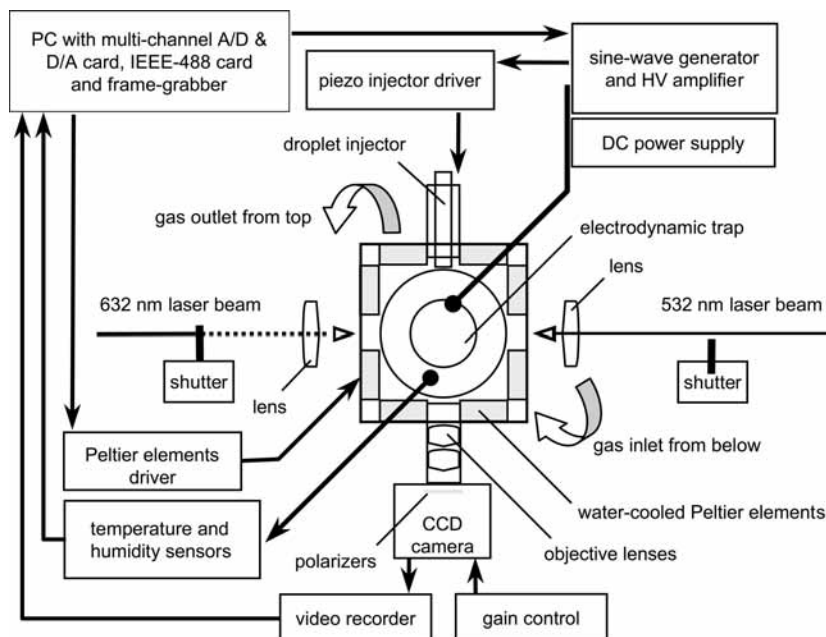


Figure 1. Experimental setup—top view.

air and for nitrogen are consistent, which also indicates that the presence of small amounts of such soluble and/or reactant gases as CO_2 in the ambient air does not influence the value of kinetic coefficients. In comparison to our previous works, we refined our data processing, which enabled us to determine the droplet radius with higher accuracy and trace its evolution with higher confidence. Smoother radius derivatives enabled us, in turn, to employ direct fitting of the model in finding the kinetic coefficients and avoid most approximations. We also operated on a larger set of experimental runs. This yielded correction of the values of kinetic coefficients that we obtained previously and revealed a different temperature dependence. These results turned out to be in excellent agreement with the results of the BC/ARI group, the values of α coincide within the temperature range from ~ 273 to ~ 281 K, and our results extending toward higher temperature follow the temperature dependence found by the BC/ARI group. Since the BC/ARI group's results and our results together span a larger temperature range, the accuracy of finding the temperature dependence of α could be improved.

2. Experimental Section

The experimental setup is presented in Figure 1. It consisted of a hyperboloidal electrodynamic quadrupole trap (see, e.g., ref 22), kept in a small climatic chamber. The high-resistivity electric circuit of the trap drive enabled us to operate in a humid atmosphere. A detailed description of this apparatus can be found in refs 21 and 23, and that of further modifications can be found in refs 24 and 25.

The droplets were introduced into the trap with a piezo injector, similar to that constructed, e.g., by Lee et al.²⁶ or Zoltan.²⁷ The injection timing was controlled relative to the trap driving AC signal. By choosing the proper injection phase, the sign and, to a certain extent, also the value of the charge of the injected droplet could be controlled. The initial temperature of the droplet was that of the chamber.

In each experiment, the chamber was first flushed with clean, dry nitrogen and then filled with a mixture of nitrogen/air and water vapor. The temperature in the chamber was monitored and stabilized. A zone-type temperature control enabled us to

eliminate vertical temperature gradients. Horizontal gradients were found to be negligible.

The humidity in the chamber but outside of the trap was monitored continuously with semiconductor sensors. Due to poor vapor exchange through trap openings accompanied by injecting liquid water into the trap, the humidity inside of the trap could not be inferred directly from those measurements. The value of the humidity in the trap found as a fitting parameter (see section 4) turned out to be higher by several percent than the sensors readings. Resorting to the fitting method was inevitable since the humidity accuracy required for the correct assessment of kinetic coefficients was inaccessible via any online sensor measurement. On the contrary, analyzing the droplet radius evolution seems to be a highly accurate method of measuring relative humidity, surpassing any online methods.

In our experiments, we used ultrapure water. The details about its initial parameters and sample preparation can be found in ref 21, where we discussed also the absorption of impurities by ultrapure water and their influence upon the experimental results there.

Droplet evolutions were studied with time-resolved static light scattering, with green or red laser light. We found no inconsistency between the results obtained for both, and we infer that the light wavelength had no influence upon the results.

3. Evaporation Model

In order to interpret the experimental results, a model of evaporation was necessary. The model of evaporation that we used was based on a generally accepted model, which can be found in such textbooks as those in refs 9, 28, and 29. It was a slightly rephrased and numerically reexamined version of what we had used previously.^{21,30} Below, we discuss the details of the model equations that we used since the results may depend significantly on the apparently minute approximations made. We also point to a certain approximation typically made that we found weighing heavily upon the results.

The quasi-stationary evaporation of a free, motionless droplet larger than the mean free path of vapor molecules can be easily described with the diffusion equations with boundary conditions

defined by the thermodynamic conditions in the reservoir (far from the droplet). This part of the model does not raise many difficulties as long as the characteristic times of the process justify the quasi-stationary approach.^{31,32}

For small droplets, of the size comparable with the mean free path of vapor molecules, the language of diffusion is not appropriate. The transport of mass and heat below the mean free path distance from the surface must be perceived as effusion or evaporation into vacuum. The net effusive flow of vapor can be expressed as the difference between outgoing and incoming effusive flows^{9,33}

$$J = \pi a^2 \alpha [\rho_e(r = a) \bar{v}(T_a) - \rho(r = a + \Delta) \bar{v}(T_{a+\Delta})] \quad (1)$$

where $\bar{v}(T) = (8RT/\pi M)^{1/2}$ is the mean absolute thermal velocity of vapor molecules for the temperature T ; T_a is the temperature of the droplet (surface), $T_{a+\Delta}$ is the temperature of the vapor at the distance Δ (comparable with the mean free path of the vapor molecule) from the surface. $\rho(r)$ is the vapor density at the distance r from the droplet center, while $\rho_e(r = a)$ is the vapor density at the droplet surface for the equilibrium conditions (steady state, no net flow).

The usual approximation made is $T_a = T_{a+\Delta}$ (see, e.g., ref 9). It implies neglecting the slowing down of the mass transport by thermal effusion (a short-range analogue of thermal diffusion). It should also be noted that lifting the temperature dependence of \bar{v} introduces some additional temperature dependence into α . Unfortunately, discarding this usual approximation excludes using standard solutions and substantially complicates calculations. To overcome such difficulties, we decided to introduce a simple correction of α at the end. We shall address this issue in detail later. Following the standard route, we compare effusive and diffusive flows at $r = a + \Delta$. Since these flows are equal and both are proportional to the vapor density gradient, it is possible to write a compact expression

$$a \frac{da}{dt} = \frac{MD_k(a, T_a)}{R\rho_L} \left[S \frac{p_\infty(T_R)}{T_R} - \frac{p_a(T_a)}{T_a} \right] \quad (2)$$

$$= \frac{MD_k(a, T_a) p_\infty(T_R)}{R\rho_L T_R} \left[S - \frac{p_a(T_a) p_\infty(T_a) T_R}{p_\infty(T_a) p_\infty(T_R) T_a} \right] \quad (3)$$

where

$$\frac{p_a(T_a)}{p_\infty(T_a)} = \exp \left[\frac{M}{RT_a \rho_L} \left(\frac{2\gamma}{a} - \frac{Q^2}{32\pi^2 \epsilon_0 a^4} \right) \right] \quad (4)$$

is the Kelvin equation, accounting for the modification of equilibrium vapor density near the droplet surface due to the surface curvature and charge effects,²⁹ and

$$\frac{p_\infty(T_a)}{p_\infty(T_R)} = \exp \left[\frac{qM}{R} \left(\frac{1}{T_R} - \frac{1}{T_a} \right) \right] \quad (5)$$

is the Clausius–Clapeyron equation. The effective diffusion coefficient D_k accounts for the effect of effusion

$$D_k = \frac{D}{a/(a + \Delta_C) + D\sqrt{2\pi M/(RT_a)}/(a\alpha)} \quad (6)$$

D is the diffusion constant for water vapor in nitrogen/air, T_R is the temperature of the reservoir, Q is the droplet charge, and p_∞ and p_a are the equilibrium (saturated) vapor pressure above the flat interface and above the interface of the curvature radius a at a given temperature. S is the relative humidity, and γ , ρ_L ,

M , and q are the surface tension, density, molecular mass, and the latent heat of evaporation of liquid water; ϵ_0 is the permittivity of vacuum, and R is the universal gas constant. The Δ_C defines the effective range of the gas kinetic effects. It is comparable with the mean free path of particles of the surrounding gaseous medium λ_a . We assumed $\Delta_C = 4\lambda_a/3$.⁹

The change of droplet mass by evaporation (condensation) is associated with heat absorption (release), which manifests as temperature drop (rise) toward the droplet. The equation for the transport of heat can be presented in a convenient form

$$a \frac{da}{dt} = \frac{\lambda_K(a, T_a)}{q\rho_L} (T_a - T_R) \quad (7)$$

where

$$\lambda_K = \frac{\lambda}{a/(a + \Delta_T) + \lambda\sqrt{2\pi M_N/(RT_a)}/(a\alpha_T \rho_N c_p)} \quad (8)$$

is the effective thermal conductivity of moist nitrogen (air) and λ , ρ_N , M_N , and c_p are thermal conductivity, density, molecular mass, and specific heat capacity under constant pressure of moist air/nitrogen, respectively. The Δ_T plays a role analogous to Δ_C and was assumed as $\Delta_T = \Delta_C + 4\lambda/(\bar{v} c_p \rho_N)$. Since in the vicinity of standard temperature and pressure the partial pressure of water vapor can be neglected in comparison to that of air/nitrogen, it can be assumed that the heat is conducted to the droplet mostly by the molecules of air/nitrogen. In consequence, the flux of mass can be considered independently of the flux of heat, and Δ_C associated with the transport of mass should be distinguished from Δ_T associated with the transport of heat.

The direct influence of the droplet charge, through charge–dipole interaction, upon the mass (or heat) transport was estimated to be negligible for droplet charge, ensuring Coulomb stability (compare with ref 34). Similarly, field emission did not take place for surface charge densities encountered in our experiments (see, e.g., ref 35). The Coulomb explosion of the droplet is a threshold process and does not need accounting in the transport equations.

4. Experimental Data Processing

The procedure of the numerical processing of experimental data, which we found to be the most stable and yield the most consistent results, relies on the direct fit of the model equations to the experimentally obtained droplet radius change rate $\dot{a} \equiv da/dt$ as a function of droplet radius a . The data preparation procedure is presented below.

The running radius of the droplet $a_i(t_i)$ was obtained (off line) from the angularly resolved Mie scattering pattern for the time t_i with the help of a gradientless fitting procedure (“library method”). Each droplet evolution yielded a sequence of a few hundreds of data points indexed with i (see Figure 2). We found that in order to obtain reliable results, significant care must be taken to ensure a high signal-to-noise ratio of the measurement. There happened to be data points misplaced to the incorrect “evolution branch”, associated with the Mie resonances that could not be handled with the method used (see a description of the method²¹). The accuracy of a single value of the droplet radius a_i (except for misplaced points) was estimated as ± 15 nm. The $a_i(t_i)$ sequence was stripped to the main “evolution branch” (indicated with the arrow in Figure 2) and interpolated in order to obtain regularly spaced data points. The time derivative $\dot{a}_i(t_i)$ was calculated (Figure 2). The $a_i(t_i)$ evolution was smoothed with a low-pass FFT filter and combined with

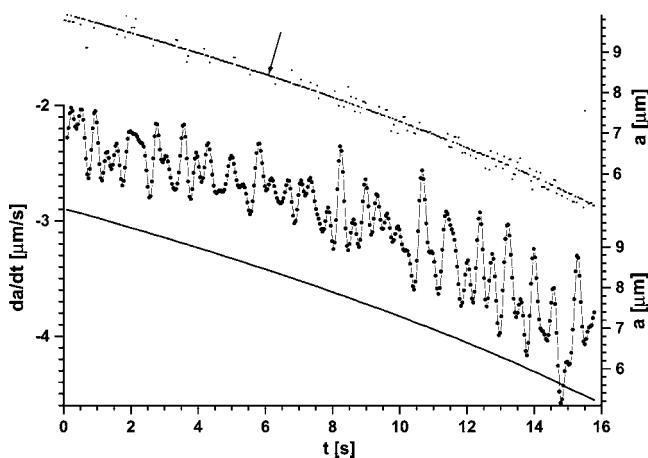


Figure 2. An example of temporal droplet radius evolution, before and after processing (top and bottom curve, respectively). Derivative calculated from processed data (middle curve); $N = 395$, $T_R = 283$ K, $p_{\text{atm}} = 1006$ hPa, $S_{\text{sens}} = 0.9$.

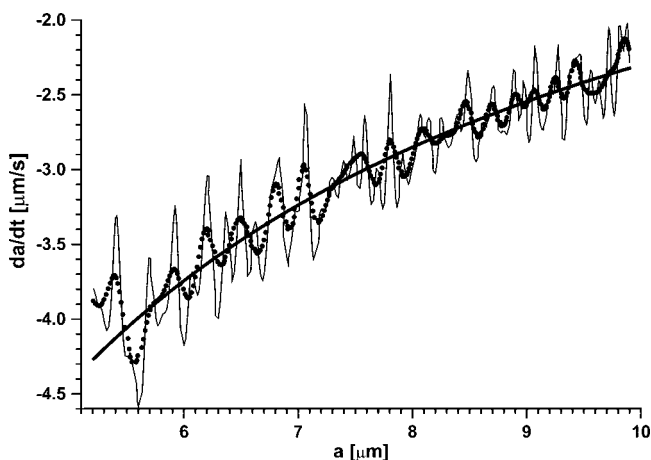


Figure 3. Droplet radius temporal derivative versus droplet radius, corresponding to Figure 2, before and after filtering (points). The result of model fitting is represented by the solid line. Fitting parameters: $S_{\text{fit}} = 0.9762$, $Q = 3.7 \times 10^6$ elementary charge units, $\alpha = 0.155$, $\alpha_T = 1$.

the derivative in order to obtain $\dot{a}_i(a_i)$. Finally, $\dot{a}_i(a_i)$ was smoothed (Figure 3).

On the other hand, subtracting eq 2 from eq 6 leads to an equation binding T_a and a . For every experimental a_i , this equation can be unambiguously numerically solved for T_a , yielding $T_a(a_i)$. This, upon insertion into eq 2, yields at every experimental data point a numerically solvable equation binding \dot{a} and a_i . Thus, a model prediction of $\dot{a}(a_i)$ could be obtained.

In order to find α , α_T , S , and Q , we minimized the function

$$\chi^2 = \frac{\chi_0^2}{N} \sum_{i=1}^N [\dot{a}_i(t_i) - \dot{a}(a_i(t_i), \alpha, \alpha_T, S, Q)]^2 \quad (9)$$

using a gradient method. N is the total number of experimental data points of the evolution, and χ_0 is an arbitrarily chosen normalizing factor. The α and S were found to be the essential parameters and could be unambiguously determined, while α_T and Q could be determined only with limited confidence. Since α and S had seemed partially interconnected, the minimization was performed very carefully, starting from various combinations of α and S (α larger, S smaller versus α smaller, S larger), and accepted only if leading to the same results. The less relevant parameters were initialized as follows: $\alpha_T = 1$ (values above 1 were allowed; compare with ref 12) and $Q = 8\pi(\epsilon_0\gamma a_i^3)^{1/2}$

2, where a_i corresponded to the smallest droplet radius observed in the evolution (no Coulomb instabilities during evolution). The resulting Q was very approximate, and we could not detect the eventual droplet charge loss (see, e.g., ref 36) by analyzing the evolution of the droplet radius. The minimization was also hardly sensitive to α_T ; however, a value close to unity could be inferred. Since for larger droplets ($a > 6 \mu\text{m}$) the kinetic effects as well as the effect of the droplet charge were negligible, only S was fitted in this range as a first step, and then, the minimization was extended toward smaller radii, with α added as a parameter. Finally, α_T and Q parameters were added. The whole procedure exhibited the best stability for $S > 95\%$ since the evaporation was slower then (compare eq 2), and thus, (i) the evolution of the droplet radius could be determined with high precision and (ii) the temperature jump at the interface ΔT was so small (compare eq 6) that the model equations used were exact enough. It would be valuable to validate the procedure of finding kinetic coefficients using other liquids (such as ethylene glycol). Unfortunately, the parameters such as the diffusion constant are usually not known with adequate precision. On the other hand, after slight modification of the procedure, it should be possible to look just for the diffusion constant, which we intend to do soon.

4.1. Correction of α . In order to estimate the influence of ΔT upon the obtained value of α , we apply an approximation $T_{a+\Delta} = T_R$ to eq 1, which is opposite to the usually applied $\Delta T = 0$, and we compare the results of both approximations. The approximation that we introduce means that we account only for thermal effusion while neglecting thermal diffusion. Since for our experimental conditions the temperature gradient was highest in the very vicinity of the interface (see ref 37), our approximation was legitimate. For simplicity, we also assumed that the shape of the distribution of the vapor density was spatially constant and temperature independent. It implied that $\rho(r = a + \Delta) = S_{a+\Delta}\rho(T_R)$, where $S_{a+\Delta} = \text{const}$ represented the relative humidity at $r = a + \Delta$. If we require that the effusive flows calculated with each of the approximations are equal, we have

$$\frac{\alpha}{\alpha(\Delta T = 0)} = \frac{S_{a+\Delta} - \frac{\rho_c(T_a)}{\rho_c(T_R)} \sqrt{\frac{T_R}{T_a}}}{S_{a+\Delta} - 1} \approx \frac{S_{a+\Delta} - \frac{\rho_c(T_a)}{\rho_c(T_R)}}{S_{a+\Delta} - 1} \quad (10)$$

Introducing $T_a(a_i)$ (see section 4) into eq 10, we can find a correction of α , where $S_{a+\Delta}$ is a (scaling) parameter. It is initiated as $S_{a+\Delta} = S$ and optimized so that $\alpha/\alpha(\Delta T = 0) \rightarrow 1$ for $\Delta T \rightarrow 0$ (larger T_a in the case of our experiment; see the inset in Figure 4). The results presented in Figure 5 are already corrected. In our case, a significant (by a factor of nearly 2) correction was near the freezing point and by several percent at 276.5 K. Equation 9 is essentially approximate and leads to underestimation of α . It can be seen in Figure 5 that our data points seem to lie slightly below the trend line. It turns out that for many reasonable experimental conditions, the correction factor can be higher than 2. We shall discuss a few examples in section 5.1. Considering the approximations made, we estimate that for thermodynamic conditions encountered in the atmosphere, the accuracy of the correction factor should not be worse than several percent.

5. Results and Discussion

The raw results are presented in Figure 4 as a function of the droplet (surface) temperature. The kinetic coefficients should

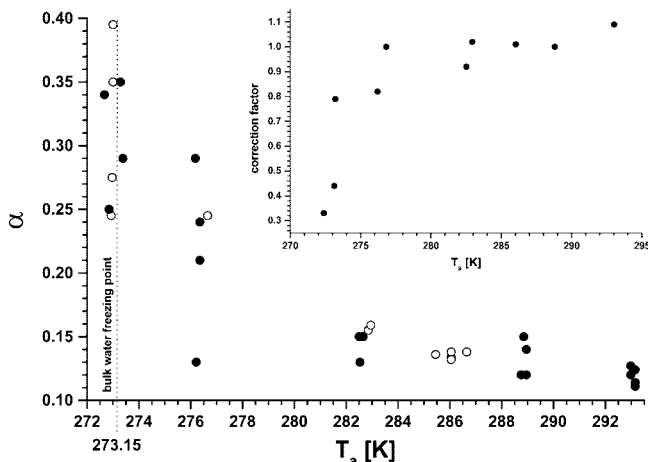


Figure 4. Nonaveraged experimentally obtained values of α as a function of droplet surface temperature. Solid and open circles represent results obtained for nitrogen and air, respectively. The corresponding calculated evaporation coefficient correction factors, due to the thermal effusion, are presented in the inset.

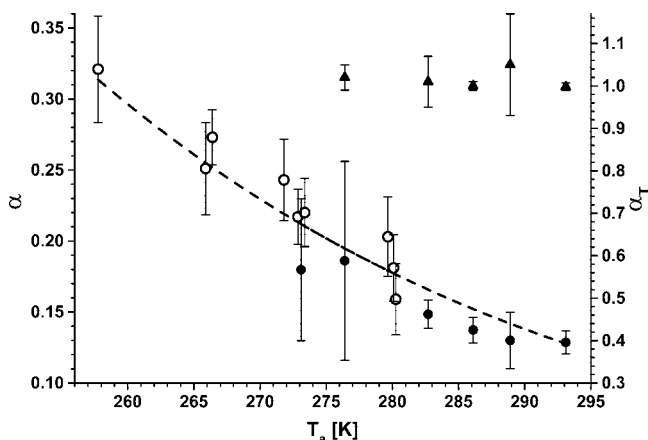


Figure 5. Collected α and α_T values as a function of droplet surface temperature. Solid circles and triangles are the corrected evaporation coefficient and thermal accommodation coefficient, respectively, obtained from our measurements; hollow circles are condensation coefficient measured by the BC/ARI group.¹ The dashed line represents the fit of eq 11 to the results of the BC/ARI group and our data together.

be presented as a function of the droplet (surface) temperature since, in general, due to evaporative cooling, it may differ significantly from the temperature of the reservoir. In case of the BC/ARI group experiments, $T_R - T_a \leq 2$ K.³¹ Though, in our case, $T_R - T_a \leq 0.7$ K only, and it is sufficient that some of our results correspond to supercooled water as well.

The kinetic coefficients found for water droplets in nitrogen and in air were mutually compatible (see Figure 4). It implies that the gases absorbed by water from the air had negligible impact upon our measurements, and generally, there is no strong dependence upon the composition of the ambient atmosphere.

The final results are shown in Figure 5. There are values of the evaporation coefficient that we obtained (solid circles) and values obtained by the BC/ARI group taken from ref 1 (hollow circles). The values of the thermal accommodation coefficient that we obtained are also presented (solid squares). Data points corresponding to our results were obtained by averaging the raw results (compare Figure 4). We also followed the BC/ARI group and used the formula that they derived based on transition-state theory (TST) (e.g., eq 7 in ref 38). Such formulation

enables expressing of the results in the language of thermodynamic potentials

$$\frac{\alpha}{1 - \alpha} = \exp(\Delta G_{\text{obs}}) \quad (11)$$

where ΔG_{obs} is the Gibbs free energy, and its temperature dependence can be expressed as $\Delta G_{\text{obs}} = \Delta H_{\text{obs}} - T\Delta S_{\text{obs}}$. ΔH_{obs} and $T\Delta S_{\text{obs}}$ are treated just as parameters; their physical meaning is not clear (see discussion below). This formula is derived on an assumption, well justified with elegant experiments by Nathanson et al. described in ref 38, that the particles from the gaseous phase enter the liquid via an intermediate surface state. The dashed line in Figure 5 represents the fit that we made to the results of the BC/ARI group and our data points together. It yielded $\Delta H_{\text{obs}} = 4830 \pm 150$ cal/mol and $\Delta S_{\text{obs}} = 20.3 \pm 0.5$ cal/mol, which is within the limits of error equal to the values given in ref 1, that is, $\Delta H_{\text{obs}} = 4.8 \pm 0.5$ kcal/mol and $\Delta S_{\text{obs}} = 20.3 \pm 1.8$ cal/mol. The accuracy of our fit (and also of the values obtained) is higher due to the larger number of data points.

The comparison of our results with those of the BC/ARI group indicates also that there was no perceivable influence of droplet charge upon kinetic coefficients. The vibrating orifice injector generates, at least on average, neutral droplets, while in our experiments with evaporating charged droplets, it could be assumed that the charge was approaching its maximum value, the Rayleigh limit. Similarly, the comparison of the aforementioned experiments reveals no measurable influence of the ambient atmosphere pressure upon the values of the kinetic coefficients.

The temperature dependence of α , though obtained with an essentially different method, coincides with the results of the BC/ARI group (see, e.g., ref 20). Our result extends into a higher temperature range. Furthermore, we measured the evaporation coefficient, while the BC/ARI group measured the condensation coefficient. It supports the notion of equivalence of these coefficients.

The thermal accommodation coefficient that we obtained, $\alpha_T = 1 \pm 0.05$ (Figure 5), agrees with both the BC/ARI and the UV/UH groups' results. However, it is hard to assess the real uncertainty of α_T ; the statistical error that we found may be too small (see section 4). Thus, it is not possible to derive information on its temperature dependence. Recently, there seems to arise a general consensus that α_T is close to 1, which means that all of the particles striking the interface thermalize.

5.1. An Attempt of Results Coordination. Since it is quite improbable that all of the kinetic coefficients measurements performed over the years were loaded with random errors, it must be assumed that the experiments, though accurate by themselves, measured different quantities. Many authors have tried to coordinate the results by pointing out what was really measured (see, e.g., refs 9 and 11). However, there is no consensus. We shall also try to address this issue.

The divergence of results obtained by different authors has been usually attributed to (i) difficulties in accounting for various physical and chemical interfacial processes; (ii) effects of impurities and especially surface-active agents;³⁹ (iii) the structure of the interface (dynamic surface tension, reaching the balance by the interface); and (iv) dependence of the coefficient value upon the model used (indirectness of measurement). It has been pointed out^{9,11} that two classes of experiments could be distinguished: (i) with a quasi-static interface, yielding $\alpha < 0.1$ and (ii) with a continuously renewing surface, yielding $\alpha \geq 0.1$. However, such categorization requires defining the

time scale. Such a scale has not been agreed to yet, and neither has the leading mechanism responsible for interface aging. For example, the characteristic times used in molecular dynamics (MD) studies are only hundreds of picoseconds. This falls into a nonstationary interval, when the transients in the temperature and vapor density fields are starting to form. The TST considerations of Nagayama et al.⁴⁰ seem to be in agreement with MD calculations and predict $\alpha \approx 1$ at around room temperature. However, it is worth noting that, for example, stationary values of the surface tension are reached within milliseconds¹¹ and all of these time scales are far below the characteristic time scale of cloud droplet growth processed, which lie in the range of seconds (or even minutes).⁴¹

Recently, Fukuta and Myers¹⁷ have noticed that accounting for the effect of moving the gas–liquid interface (“moving boundary effect”) can change the resulting value of the kinetic coefficients by several percent. In their work, they managed to account for this effect in an elegant way. Although the thermodynamical conditions and the velocity of the interface in our experiment were similar to theirs, in the present work, we have decided to neglect the moving boundary effect since the correction of the mass accommodation coefficient that we propose is much larger.

In this paper, we would like to point to a mechanism which falls within the fourth category, the model-dependent mechanism; however, it is related to the issue of the characteristic time scale of the process and its distance from the thermodynamic equilibrium. Usually, authors are careful to estimate the characteristic times of mass and heat transport processes involved in order to ensure the proper description. It seems that in some cases, this alone can be somewhat misleading because of the thermal effusion that we already mentioned. We shall consider four examples.

In case of the BC/ARI group experiments, the vapor–liquid contact lasts several milliseconds, but the droplet is essentially in equilibrium with the reservoir. In order to achieve temperatures below 273 K, evaporative cooling was used, which inevitably caused a temperature jump near the surface (up to 2 K) and thermal effusion as a consequence. However, since the value of α was not obtained from the evolution of the droplet radius, its value should be safe, and no correction is needed.

In our case, we selected for the analysis the droplet evolutions that lasted a few seconds, which guaranteed that the process had been quasi-stationary in the diffusion time scale. For faster evolutions, the temperature jump approached 1 K, and since α was obtained from the evolution, it had to be corrected by means presented above.

In case of the experiment of the UV/UH group,¹² the evolution lasted ~ 50 ms, which is shorter than that in our case, but for the thermodynamic conditions that they had, the process still could be regarded as quasi-stationary. However, the temperature jump of ~ 3 K could be expected for such an evolution. This alone would require a correction of α by a factor of 2. Further overestimation might be caused by the uncertainty of water vapor saturation. There are also rather few data points lying on a relatively flat curve, which, as we know from our experience, causes the increase of the measurement uncertainty.

Lastly, in case of the very interesting Fukuta and Myers experiment,¹⁷ the evolution (condensation) lasted ~ 3 s (similar to that in our experiment). Since the final droplet radius was $\sim 2 \mu\text{m}$, it can be inferred that $\dot{a} \approx 1 \mu\text{m/s}$, which in turn yields a temperature jump of only ~ 0.2 K. However, since the mass transport was relatively slow (supersaturation used was very small), the effect of even a small temperature jump at the

interface could be relatively large. According to our estimation (see eq 10), the correction of the mass accommodation coefficient should be as high as 5! This would bring Fukuta and Myers’s result for NaCl and $(\text{NH}_4)_2\text{SO}_4$ at 277 K to $\alpha \approx 0.2$, which agrees within the limits of error with ours and the BC/ARI group results, even allowing for the moving boundary effect that we neglected.

6. Conclusions

We conclude that it is feasible to obtain reliable values of the evaporation coefficient by analyzing the evaporation of a small droplet. It requires however several tens of data points per evolution and droplet radius measurement accuracy of several nanometers. The generally accepted model of quasi-stationary evaporation seems sufficient for experimental data analysis in most cases. We found however that when evaporative cooling of the droplet becomes of the order of 1 K, it is necessary to consider the effect of thermal effusion, which is a short-distance analogue of thermal diffusion. The kinetic coefficients found for water droplets in nitrogen and in air were mutually compatible. The evaporation coefficient for the temperature range from 293.1 K down to 273.1 K was found to increase from ~ 0.13 to ~ 0.18 and follow the trend given by the Arrhenius formula (see eq 11) with the parameters $\Delta H_{\text{obs}} = 4830 \pm 150$ cal/mol and $\Delta S_{\text{obs}} = 20.3 \pm 0.5$ cal/mol. This temperature dependence is in excellent agreement with the results of the BC/ARI group, which concern the condensation coefficient, that were obtained with an essentially different technique for a much lower ambient gas pressure and that extend toward lower temperatures. The comparison with the BC/ARI group experiments enables us to draw a few additional conclusions: (i) the evaporation and condensation coefficients are essentially equivalent; (ii) there was no measurable influence of ambient atmosphere pressure upon the value of the kinetic coefficients in the range from ~ 1 to ~ 100 kPa; and (iii) there was no measurable influence of droplet charge on the value of the kinetic coefficients up to the Rayleigh stability limit. The value of the thermal accommodation coefficient that we obtained, $\alpha_T = 1 \pm 0.05$, agrees well with recent results of many authors.

Acknowledgment. This work was supported by the Polish Ministry of Science and Higher Education Grant No. 1 P03B 117 29.

References and Notes

- (1) Li, Y.; Davidovits, P.; Shi, Q.; Jayne, J.; Kolb, C.; Worsnop, D. *J. Phys. Chem. A* **2001**, *105*, 10627.
- (2) McFiggans, G.; Artaxo, P.; Baltensperger, U.; Coe, H.; Facchini, M.; Feingold, G.; Fuzzi, S.; Gysel, M.; Laaksonen, A.; Lohmann, U.; Mentel, T.; Murphy, D.; O’Dowd, C.; Snider, J.; Weingartner, E. *Atmos. Chem. Phys. Discuss.* **2005**, *5*, 8507.
- (3) Laaksonen, A.; Vesala, T.; Kulmala, M.; Winkler, P.; Wagner, P. *Atmos. Chem. Phys. Discuss.* **2004**, *4*, 7281.
- (4) Ackerman, A.; Toon, O.; Hobbs, P. *J. Atmos. Sci.* **1995**, *52*, 1204.
- (5) Grimm, R.; Beauchamp, J. *Anal. Chem.* **2002**, *74*, 6291.
- (6) Sazhin, S. *J. Phys.: Conf. Ser.* **2005**, *22*, 174.
- (7) Perçin, G.; Khuri-Yakub, B. *Rev. Sci. Instrum.* **2002**, *74*, 1120.
- (8) Sommerfeld, M.; Qui, H.-H. *Int. J. Heat Fluid Flow* **1998**, *19*, 10.
- (9) Pruppacher, H.; Klett, J. *Microphysics of Clouds and Precipitation*; Kluwer: Dordrecht, The Netherlands, 1997.
- (10) Shi, Q.; Davidovits, P.; Jayne, J.; Worsnop, D.; Kolb, C. *J. Phys. Chem. A* **1999**, *103*, 8812.
- (11) Marek, R.; Straub, J. *Int. J. Heat Mass Transfer* **2001**, *44*, 39.
- (12) Winkler, P.; Vrtala, A.; Wagner, P.; Kulmala, M.; Lehtinen, K.; Vesala, T. *Phys. Rev. Lett.* **2004**, *93*, 75701/1.
- (13) Hagen, D.; Schmitt, J.; Trublood, M.; Carstens, J.; White, D.; Alofs, D. *J. Atmos. Sci.* **1989**, *46*, 803.

- (14) Zagaynow, V.; Nuzhny, V.; Cheusova, T.; Lushnikov, A. *J. Aerosol Sci.* **2000**, *31*, S795.
- (15) Sageev, G.; Flagan, R.; Seinfeld, J.; Arnold, S. *Colloid Interface Sci.* **1986**, *113*, 421.
- (16) Gollub, J.; Chabay, I.; Flygare, W. *J. Chem. Phys.* **1974**, *61*, 2139.
- (17) Fukuta, N.; Myers, N. M. *J. Atmos. Sci.* **2007**, *64*, 955.
- (18) Shaw, R.; Lamb, D. *J. Chem. Phys.* **1999**, *111*, 10659.
- (19) Xue, H.; Moyle, A.; Magee, N.; Harrington, J.; Lamb, D. *J. Atmos. Sci.* **2005**, *62*, 4310.
- (20) Davidovits, P.; Worsnop, D.; Jayne, J.; Kolb, C.; Winkler, P.; Vrtala, A.; Wagner, P.; Kulmala, M.; Lehtinen, K.; Vesala, T.; Mozurkewich, M. *Geophys. Res. Lett.* **2004**, *31*, L22111/1.
- (21) Jakubczyk, D.; Zientara, M.; Kolwas, K.; Kolwas, M. *J. Atmos. Sci.* **2007**, *64*, 996.
- (22) Major, F. G.; Gheorghe, V. N.; Werth, G. *Charged Particle Traps*; Springer: Berlin, Germany, 2005.
- (23) Jakubczyk, D.; Zientara, M.; Bazhan, W.; Kolwas, M.; Kolwas, K. *Opto-Electro. Rev.* **2001**, *9*, 423.
- (24) Jakubczyk, D.; Derkachov, G.; Bazhan, W.; Łusakowska, E.; Kolwas, K.; Kolwas, M. *J. Phys. D* **2004**, *37*, 2918.
- (25) Jakubczyk, D.; Derkachov, G.; Zientara, M.; Kolwas, M.; Kolwas, K. *J. Opt. Soc. Am. A* **2004**, *21*, 2320.
- (26) Lee, E.; Perl, M. Universal Fluid Droplet Ejector. Patent # 5943075, 1999.
- (27) Zoltan, S. Pulsed Droplet Ejecting System. Patent # 3683212, 1972.
- (28) Fuchs, N. *Evaporation and Droplet Growth in Gaseous Media*; Pergamon: London, 1959.
- (29) Friedlander, S. *Smoke, Dust and Haze Fundamentals of Aerosol Dynamics*; Oxford University Press: New York, 2000.
- (30) Zientara, M.; Jakubczyk, D.; Derkachov, G.; Kolwas, K.; Kolwas, M. *J. Phys. D* **2005**, *38*, 1978.
- (31) Worsnop, D.; Zahniser, M.; Kolb, C.; Gardner, J.; Watson, L.; Van Doren, J.; Jayne, J.; Davidovits, P. *J. Phys. Chem.* **1989**, *93*, 1159.
- (32) Schwartz, S.; Freiberg, J. *Atmos. Environ.* **1981**, *15*, 1129.
- (33) Present, R. *Kinetic Theory of Gases*; McGraw-Hill: New York, 1958.
- (34) Nadykto, A. B.; Yu, F. *Atmos. Chem. Phys. Discuss.* **2003**, *3*, 4927.
- (35) Gamero-Castaño, M. *Phys. Rev. Lett.* **2002**, *89*, 147602/1.
- (36) Duft, D.; Lebius, H.; Huber, B.; Guet, C.; Leisner, T. *Phys. Rev. Lett.* **2002**, *89*, 84503/1.
- (37) Fang, G.; Ward, C. *Phys. Rev. E* **1999**, *59*, 417.
- (38) Nathanson, G.; Davidovits, P.; Worsnop, D.; Kolb, C. *J. Phys. Chem.* **1996**, *100*, 13007.
- (39) Feingold, G.; Chuang, P. *J. Atmos. Sci.* **2002**, *59*, 2006.
- (40) Nagayama, G.; Tsuruta, T. *J. Chem. Phys.* **2003**, *118*, 1392.
- (41) Chuang, P.; Charlson, R.; Seinfeld, J. *Nature* **1997**, *390*, 594.

JP7114324